Modeling of Asphalt Pavement Surface Temperature for Prevention of Icing on the Surface

Hüseyin AKBULUT[1]
Lale ATILGAN GEVREK[2*]
Murat AY[3]

ABSTRACT

Hydronic heating systems are emerging as one of the best methods, which are environmentally friendly, clean, and sustainable modern ice prevention methods, an alternative to traditional ice precautions in the pavements. In this present study, temperatures were measured on asphalt samples prepared using the hydronic heating system when the air temperature in situ fell below 0 °C. T (minute), the temperature of influent (°C), air temperature (°C), temperature of effluent (°C) and pavement mean temperature (°C) were measured for four different asphalt samples. The results of the measurements were then modeled separately for four samples (345×4=1380 data) by using multiple linear regression (MLR), multi-layer perceptron (MLP), and radial basis neural network (RBNN). The results were discussed as tables and graphs. The performances of the models were evaluated using the root mean square error (RMSE), mean absolute error (MAE), and determination coefficient (R^2). According to the results, the RBNN models of four inputs had the best performance for each sample. The RBNN (4,0.6,9) model, which refers to 4-inputs, spread coefficient of 0.6 and hidden nodes of 9, of sample-3 with RMSE=0.76 °C and MAE=0.63 °C and R^2=0.91 had the best performance among all models. In addition, it is thought that the models having low errors in this concept can be evaluated for early warning systems for the ice condition of the roads.

Keywords: Ice prevention, modeling of pavement temperature, traffic safety.

1 Afyon Kocatepe University, Department of Civil Engineering, Afyonkarahisar, Türkiye
  hakbulut@aku.edu.tr - https://orcid.org/0000-0003-4504-4384

2 Yozgat Bozok University, Department of Construction Technologies, Yozgat, Türkiye
  lale.gevrek@bozok.edu.tr - https://orcid.org/0000-0003-2015-9679

3 Yozgat Bozok University, Department of Civil Engineering, Yozgat, Türkiye
  murat.ay@bozok.edu.tr - https://orcid.org/0000-0002-7222-7912

* Corresponding author

1. INTRODUCTION

Snow and icing cause unsafe pavement surfaces for both pedestrians and motor vehicle traffic. At the same time, the chemicals used for defrosting or prevention both harm to the environment and create an economic burden to the countries [1, 2, 3, 4, 5, 6]. As another method for anti-icing on the pavements, hydronic heating systems have been used in many countries. This system circulates a heated fluid through a network of pipes placed under the pavement to melt the snow and ice in the pavement, and this liquid is a solution of salt and water or liquids such as oil and glycol [7]. The pipe network usually consists of systems laid in a crimped configuration. The material of the pipe is usually cross-linked or high-density polyethylene. Typical pipe ranges from 150 to 300 mm and depth from 50 to 75 mm. Nominal pipe diameters are usually between 18 and 25 mm. Various liquids such as saltwater, oils and glycol water are suitable as heat carrier fluids in hydronic heating systems. The heat source to be used for hydronic heating systems is an important choice [8]. Some sources such as boilers, electric heaters, groundwater, and ground source heat pumps can be used for such systems [9, 10]. Pipe materials used to convey hot water are metal or plastic. Steel, iron, and copper pipes have been widely used over the past years; however, these pipes are corroded easily. Therefore, plastic pipes are now more widely used, and the life span of such plastic pipes is more than 50 years [11, 12, 13, 14, 15].

The icing occurs as a result of frost, fog passing over a cold road surface, groundwater seepage or melting snow, and freezing with precipitation. In addition, when the snow height reaches approximately 5 cm, it is necessary to remove the snow from the road surface. If the necessary snow control is not achieved, the accumulated snow can become the compressed form under traffic loads and turn into an ice sheet. In addition, because bridges and viaducts are built independently from the soil, they are affected by icing much faster than other highway elements depending on the atmospheric conditions. These different road conditions are very critical and may cause heavy traffic accidents that may cause pecuniary loss and intangible damages [13, 16, 17, 18].

As it can be understood from these studies, it is very important to prevent or reduce icing on the road surface in real applications. From a theoretical point of view, some modeling studies have been implemented on hydronic heating systems and the normal pavements. For example, Chiasson et al. [19] examined a design and simulation tool to model the performance of a hydronic heating system. A sample application was simulated to demonstrate the feasibility of the heating system. Minhoto et al. [20] proposed that a three-dimensional finite element model was developed to calculate the temperature of a pavement located in northeast Portugal. Liu et al. [21] performed an experimental validation for the numerical model in an experimental setup to melt the snow on the road. The model can estimate snow, ice and water conditions of snowmelt on hydronic heated pavements. Liu et al. [22] defined a numerical model of a heated pavement and the snow melting processes occurring on its surface. A set of boundary conditions that allow the treatment of various surface and weather conditions associated with storm events were defined. Wang and Chen [23] investigated the mechanism of the critical free area ratio during snowmelt pavement and the factors affecting it, using fluids such as geothermal water and industrial wastewater. A simplified theoretical model is presented to explain the heat and mass transfer process on the coating. They found that the model was effective for predicting the critical free area ratio in the snowmelt process. Xu and Tan [24] developed a heat and mass-related model for

pavement snow melting systems using low-temperature heating fluids. They used this model to simulate the performance of hydronic heated pavement using the HVACSIM Plus program. Xu et al. [14] developed a two-dimensional heat and mass coupled model for hydronic heated pavements. The numerical algorithm can calculate the surface condition, temperature/moisture content in the coating profile. Mirzanamadi et al. [25] developed a two-dimensional numerical model to investigate how different design options affect the efficiency of hydronic heating coating systems. Meteorological data from the Östersund region of Sweden were used, and they found that the distance between pipes had a significant effect on reducing icing. Johnsson and Adl-Zarrabi [26] made a numerical model for designing low temperature (4-8°C) hydronic heated pavements. The model was validated with an experimental setup. They found that the developed model can be estimated with an RMSE<1.4 °C for surface temperatures and RMSE <0.4 °C for the effluent water temperature in the behavior of a hydronic heating system. In our study, the best estimation model (RBNN(4,0.6,9)) of the asphalt surface temperature gave RMSE=0.76 and MAE=0.63. Chen et al. [27] proposed a comprehensive review of existing models developed for predicting pavement temperature and discussed the effective variables in modeling of pavement temperature. Zeiada et al. [28] studied the effect of different design factors on asphalt pavement performance in cold regions by climate factors, such as temperature and precipitation. They determined the most significant design factors prevailing in cold climate conditions. Mirzanamadi et al. [29] examined the applicability of a hydronic heated pavement system for the creation of road surfaces that store solar energy and prevent icing in summer. A hybrid 3D numerical simulation model was used to analyze solar energy storage and anti-icing processes. Climate data were obtained in Östersund, Sweden. The proposed system could reduce the slippery time of road surfaces by up to 85%. Zhao et al. [30] implemented a hydronic snow melting system in Harbin, China. According to the experimental results, a two-dimensional model was developed. For the first time, the snow microstructure was considered in the model for the hydronic snow melting system. Three variables (buried pipe depth, buried pipe spacing, and supplied fluid temperature) were compared and analyzed to optimize the design of the hydronic snowmelt system in cold regions. They found that the snow can be cleared in about 4.5 hours (270 minutes). Marcelino et al. [31] designed a general approach for the development of pavement performance prediction models using machine learning techniques. Rigabadi et al. [32] developed the pavement temperature prediction models based on remote sensing data, multiple linear/non-linear regression and artificial neural network by using variables such as air temperature, solar radiation, wind speed, and humidity. Tabrizi et al. [33] developed a new model for hourly real-time forecasting of pavement temperatures. Zhao et al. [30] developed a temporary two-dimensional model to analyze the effects of three main variables to optimize the design of a hydronic snowmelt system. One of them is the inlet water temperature. In our study, it has also been revealed that the inlet water temperature is an important variable in the estimation of asphalt pavement temperature. Xu and Tan [24] emphasized that the ambient temperature and the heating fluid temperature are the two main factors in the snow melting performance.

The properties of the hydronic heating systems were tested both in the above-mentioned studies and in a thesis [15]. At this point, it was thought that these models obtained from the above-mentioned previous studies could be evaluated as an alternative to the systems that estimate and warn especially about icing on the roads. It is known that hydronic heating systems are expensive in terms of system cost. However, there may be systems that are

suitable to be built based on the cost-benefit analysis. It is known that the costly part in this type of systems is the heating source. The cost can be reduced by using geothermal energy from renewable resources as a heat source. Moreover, the performance of this modeling assumption can be proven theoretically, as mentioned in the above studies. At this point, the performance of the modeling results of the samples were tested by using both classical and innovative modeling methods for four asphalt samples under real outdoor conditions. Moreover, other aims and different aspects of this study from previous studies are: to assess the accuracy of the MLR, MLP and RBNN for estimation of pavement surface temperatures; to examine model's performances using four experimental samples (345×4=1380 data), and to present a support model to the early warning systems for icing on the roads.

2. EXPERIMENTAL MATERIAL AND DATA

The experiment results of four asphalt samples were used in the modeling. These samples were prepared to verify the samples' behaviors in the equivalentenvironmental conditions. Also, the four same samples were prepared to verify and compare the experiment's results. Metal molds in the form of 40x40x20 cm were prepared. After the four asphalt samples were prepared, they were brought to the laboratory. An electric combi boiler was used as a heat source for the water to circulate in the system, placed in the laboratory to simulate the geothermal energy. The capacity of the combi boiler was of 24 kW. 18 mm diameter pe-x pipes were used in the hydronic heating system. Pipes were placed at 15-cm spacing. Photos of the asphalt samples are shown in Figure 1.

Figure 1 - Preparation of asphalt samples with hydronic heating system

The pipe spacing used in the sample studies was determined in accordance with that in the literature. Mold dimensions were decided by considering the determined pipe spacing. A larger size was not considered due to difficulties in the manufacturing and transportation processes. The snow-covered sections was photographed shortly after the start of the heating as shown in the figure. After a certain period of time, there were no snow-covered areas. Ice melting time was not taken into account in the study. Because the system is being operated before the air temperature drops below zero (0) degree Celsius, ice formation is not foreseen.

Pe-x pipes are manufactured by crosslinking high density polyethylene molecules. Cross-links also increase the temperature and compressive strength of the material. Pe-x cross-linked polyethylene pipes can be used for applications where flexibility as well as long-term resistance to high temperature and pressure is required. The parts of the pipes in situ the laboratory were wrapped with insulation material. Similarly, when hot water was circulated in the hydronic system inside the asphalt samples, the four sides and the bottom of the asphalt samples were wrapped with insulation materials. It is thought that the use of hydronic heating system on asphalt pavement roads can prevent low-temperature cracks that will occur as a result of the reduction of tensile stresses occurring in the wear layer in the heated superstructure and thus contribute positively to the service life. The experimental setup in the laboratory is shown in Figure 2.

Figure 2- The experimental setups in the laboratory in below 0 °C

Figure 3 - Measurements of asphalt surface temperatures with thermocouples

During the datasets acquisition process, one data logger and eight thermocouples measuring temperature were used for the measurements of asphalt surface temperature, air temperature, and influent and effluent water temperatures. The measurements were made on four asphalt pavement samples with a hydronic heating system, using water inlets at 30-40 °C water temperatures for about 2-hour in real weather conditions. The measurements were taken

when the air temperature was below 0°C. To measure the surface temperature of the asphalt samples, four thermocouples were placed at the corner points and one thermocouple was placed at the midpoint of the asphalt surface (see Figure 3). At the same time, influent water temperature, effluent water temperature, and air temperature measurements were made with a thermocouple, as can be seen in Figure 3. The data was then stored into the personal computer.

In order to model the pavement, mean temperature (°C), the experimental variables, T (minute), the temperature of influent (°C), air temperature (°C) and temperature of effluent (°C), were used in the analysis. Before starting the analysis, the Pearson correlation test, which reveals the relationship between independent variable/variables and dependent variable, was performed. The test results were analyzed at the two-tailed hypothesis test and the significance level of 0.01 (1%). In this context, Table 1 shows the correlations of each independent variable with the dependent variable for all raw data (345×4=1380) of four samples. According to Table 1, the correlation coefficients (r) between time (minute), the temperature of influent, temperature of effluent and the pavement mean temperature were calculated as +0.799, +0.081, and +0.086, respectively. Accordingly, it can be said that the time has a statistically significant and strong relationship with the pavement mean temperature, and it is also statistically significant with the temperature of the influent and the effluent. Although the correlations of the temperature of influent and temperature of effluent with the pavement mean temperature had low values, they were used in the models because they were statistically significant, as stated in Table 1. A statistically significant relationship between the air temperature and the pavement mean temperature was not observed, but the physical effects of the in-situ environment were considered in the models. In this case, the error values and graphs formed by adding the air temperature to the models were examined in detail below.

Table 1- Pearson correlations matrix of the measured variables in the experiments

Variable	Independent variables				Dependent variable
	Time (minute)	Temperature of influent (°C)	Temperature of effluent (°C)	Air temperature (°C)	Pavement mean temperature (°C)
Time(minute)	1	-0.144[*]	-0.156[*]	-0.004	+0.799[*]
Temperature of influent(°C)	-0.144[*]	1	0.868[*]	0.205[*]	+0.081[*]
Temperature of effluent(°C)	-0.156[*]	0.868[*]	1	0.137[*]	+0.086[*]
Air temperature(°C)	-0.004	0.205[*]	0.137[*]	1	+0.044
Pavement mean temperature(°C)	0.799[*]	0.081[*]	0.086[*]	0.044	1

[*]: Correlation is significant at the 0.01 (1%) significance level in the two-tailed hypothesis test. The relationship of other variables with the modelled variable (pavement mean temperature (°C)) is statistically significant except for air temperature.

Basic statistics of the four asphalt samples are presented in Table 2. The high variation coefficients of pavement mean temperature can be seen for four asphalt samples. T (minute), the temperature of influent (°C), air temperature (°C), and temperature of effluent (°C) had not high variation coefficients. Air temperatures for four asphalt samples had below 0 °C. The temperature of influent (°C), temperature of effluent (°C) and pavement mean

Table 2 - Basic statistics of the variables in the experiments

		Mean	Minimum value	Maximum value	Standard deviation	Skewness coefficient	Kurtosis coefficient	Variation coefficient
Sample-1, N=345	**Time(minute)**	57.00	0.00	114.00	33.24	0.00	-1.20	0.58
	Temperature of influent (°C)	36.71	26.60	58.10	4.92	1.67	3.96	0.13
	Air temperatur (°C)	-7.50	-9.30	-5.00	0.73	-0.13	0.52	-0.10
	Temperature of effluent (°C)	33.33	23.30	51.50	4.57	1.16	2.52	0.14
	Pavement mean temperature (°C)	1.24	-7.22	6.56	3.44	-0.34	-0.59	2.79
Sample-2, N=345	**Time(minute)**	57.00	0.00	114.00	33.24	0.00	-1.20	0.58
	Temperature of influent (°C)	39.20	18.10	61.90	8.32	0.14	-0.69	0.21
	Air temperature (°C)	-6.61	-9.20	-2.20	1.45	0.12	-0.46	-0.22
	Temperature of effluent (°C)	33.28	14.70	50.50	5.26	0.65	0.47	0.16
	Pavement mean temperature (°C)	2.25	-7.58	10.12	4.14	-0.16	-0.44	1.84
Sample-3, N=345	**Time(minute)**	57.00	0.00	114.00	33.24	0.00	-1.20	0.58
	Temperature of influent (°C)	38.29	14.40	53.50	4.96	0.24	1.06	0.13
	Air temperature (°C)	-7.84	-10.10	-4.50	1.27	1.01	0.46	-0.16
	Temperature of effluent (°C)	32.50	12.30	50.90	4.17	0.72	2.86	0.13
	Pavement mean temperature (°C)	1.84	-8.08	7.94	3.65	-0.69	-0.05	1.98
Sample-4, N=345	**Time(minute)**	57.00	0.00	114.00	33.24	0.00	-1.20	0.58
	Temperature of influent (°C)	36.06	5.60	44.40	4.60	-0.57	4.13	0.13
	Air temperature (°C)	-10.75	-13.00	-6.80	1.39	0.53	0.07	-0.13
	Temperature of effluent (°C)	33.40	4.30	42.40	4.09	-0.71	6.02	0.12
	Pavement mean temperature (°C)	2.27	-10.32	11.46	4.60	-0.35	-0.14	2.02

temperature of four asphalt samples had high standard deviations. Although the variation coefficients of T (minute), the temperature of influent (°C), air temperature (°C), temperature of effluent (°C) were low, it was observed that the variation coefficients of the pavement mean temperature were high in four asphalt samples. It can be said that the variables with these statistical properties for four asphalt samples behave similarly on the pavement mean temperature. At this point, it is possible to say that the time is an important factor in the change of variability intervals (maximum and minimum). It can be said that the pavement mean temperatures for the four asphalt samples had positive values in terms of time, and 114-minute for the system was a good performance in terms of heating of the asphalt. Moreover, the correlation of time with pavement mean temperature in Table 1 is the highest value of+0.799. According to this result, it can be said that heating time (T) has a high effect on the pavement mean temperatures.

3. METHODOLOGY

Artificial neural networks (ANNs) have been used in many applications in the literature. These methods generally estimate well and produce outputs near to the measured values. However, when these methods are run with limited data, it is possible that their estimation performance may decrease. For better estimations, the databases of the models should be constantly supported with new datasets. Also, finding meaningful outputs for complex systems with low errors, even with insufficient data, are very important in the decision-making stages of engineering projects. Therefore, modelling of pavement mean temperature (°C) was done using the classical regression method with multi-layer perceptron (MLP) and radial basis neural network (RBNN) methods to find the best model having minimum error and maximum R^2 in this study. MATLAB codes written by us were used in all models, MLP and RBNN. Nonlinear methods were considered to define the best relationship amongst the variables. Moreover, normalization of the data was done between 0.2 - 0.8 in the codes, and the data were scaled to this range. Two important methods used in this study are briefly given in the following subsections [34].

3.1. Multi-Layer Perceptron (MLP)

This section presents the architecture of the network that is most commonly used with the backpropagation algorithm the multi-layer feedforward network. MLP is based on the present understanding of the biological nervous system. It is a massive parallel system composed of many processing elements connected by links of variable weights [35]. An elementary neuron with R inputs (T (minute), temperature of influent (°C), air temperature (°C), and temperature of effluent (°C)) is shown in Figure 4. Each input is weighted with an appropriate w. The sum of the weighted inputs and the bias form the input to the transfer function f. Neurons can use any differentiable transfer function f to generate their output (the pavement mean temperature (°C)). The initial assigned weights are progressively corrected during the training process. In this process, the outputs predicted by MLP are compared with known outputs, and errors are back-propagated (from right to left in Fig. 4) to determine the appropriate weight adjustments necessary to minimize errors. In this study, the Levenberg-Marquardt [36] algorithm was used for adjusting the MLP weights.
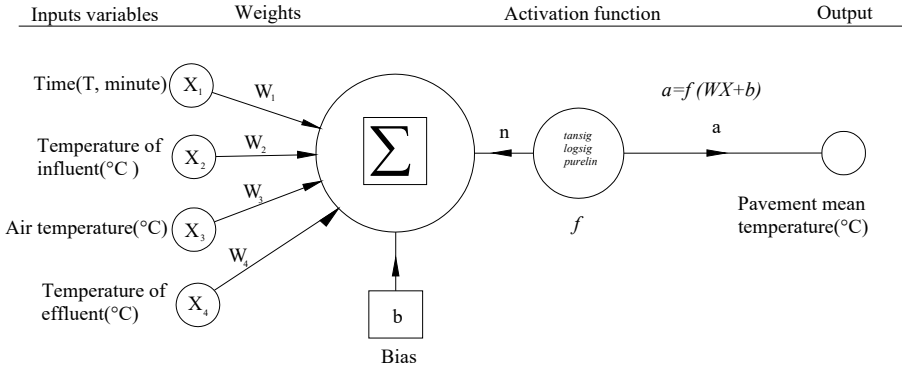
Figure 4 - Non-linear model of a neuron

In backpropagation, it is important to be able to calculate the derivatives of any transfer functions used. Each of the transfer functions above, logsig, radbas, netinv, tansig and purelin, can be called to calculate its derivative. The output of a neuron can be expressed as:

Output= f (n)

Where:

$$n = \sum_{j=1}^{R} w_j.x_j + b; \qquad x_1, x_2, x_3, ...x_R \tag{1}$$

$X_1, X_2, X_3, ..., X_R$ are the input signals; $W_1, W_2, ..., W_R$ are the weights of the neurons; b is bias value; f is activation function, R is the number of the elements in the input vector. The *tansig, netinv, tansig, logsig, purelin and tribas* are the most commonly used activation functions in artificial neural networks.

3.2. Radial Basis Neural Network (RBNN)

RBNN was first introduced into the ANNs literature by Broomhead and Lowe [37]; Poggio and Girosi [38]. The RBNN has two layers whose output nodes form a linear combination of the basis functions. RBNN is also known as a localized receptive field network because the basis functions in the hidden layer produce a significant nonzero response to input stimulus only when the input falls within a small localized region of the input space. The relation between inputs and outputs is shown in Figure 5.

The RBNN has connection weights between the hidden layer and the output layer only. These weight values can be obtained by the linear least-squares method, which gives an important advantage for convergence. The Gaussian activation function is widely used as the radial basis function. The RBNN method does not perform parameter learning as in the MLP. It performs linear adjustment of the weights for the radial bases. This characteristic gives the

9

RBNN advantage of a very fast converging time without local minima because its error function is always convex. In this study, different numbers of hidden layer neurons are examined for the RBNN models with a simple trial-and-error method. Detailed information about RBNN theory can be obtained from Haykin.
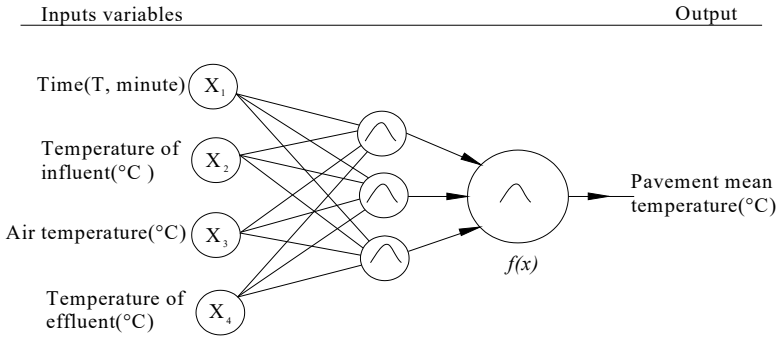

Figure 5 - Schematic diagram of RBNN architecture

4. DISCUSSIONS

To estimate pavement mean temperature, 345 experimental datasets for four samples were divided into two sets: training and testing. Approximately %70 (241) of data was randomly chosen for the training phase, %30 (104) of data was randomly chosen for the testing phase. Moreover, each sample having 345 experimental data was modeled differently and analyzed and compared, respectively, as table and graph. For the learning process for the MLP method, the inputs (T (minute), temperature of influent (°C), air temperature (°C) and temperature of effluent (°C)) and corresponding target vector (pavement mean temperature (°C)) were used to train the neural networks by applying Levenberg-Marquardt (LM) algorithm which is both fast and having the advantage in terms of gaining the time according to other training algorithms such as gradient descentand Bayesian regularization. Because the number of hidden units directly affected the performance of the network, many experimental investigations were conducted with the models. The number of intermediate layers from 1 to 20 was assayed for each model by looking at the minimum MSE values. In these analyses, one-hidden layer was enough for all models. It was found that the optimum number of hidden layers was one in all of the models for the MLP method. The stopped criteria for the training phase were MSE=0.00001 or the number of epochs of 100. The optimum transfer functions (*compet, logsig, purelin, netinv, tansig, radbas, softmax,* and *tribas*) for the MLP models were used for input and for output layers to find out the best model. Unlike the MLP, the RBNN has optimum spread; hidden node numbers are found by using a trial-error method. After the optimum spread coefficient and hidden nodes number are found, the main program is executed with these numbers. The MSE of the RBNN was taken as "0" for all of the models. Normalization of the data was done between 0.2 - 0.8 in the codes, and the data were scaled to this range. Formulas given by Eqs. 2-4 were used for the evaluation of the model's performances in the study. The root mean square error (RMSE), mean absolute error (MAE), and determination coefficient (R^2) criteria are expressed as:

$$RMSE = \sqrt{\frac{1}{N}\sum_{j=1}^{N}(Y_{measured,j} - Y_{modeled,j})^2} \tag{2}$$

$$MAE = \frac{1}{N}\sum_{j=1}^{N}\left|Y_{measured,j} - Y_{modeled,j}\right| \tag{3}$$

$$R^2 = 1 - \frac{\sum_{j=1}^{N}\left[(Y)_{measured,j} - (Y)_{modeled,j}\right]^2}{\sum_{j=1}^{N}\left[(Y)_{measured,j} - (\overline{Y})_{mean\ measured}\right]^2} \tag{4}$$

Table 3 - RMSE, MAE and R² values of the MLR, MLP, and RBNN in training and testing phases for sample-1

Comb. No.	Inputs	Target (output)	Model and optimum transfer functions	Training (N=241)			Testing (N=104)		
				RMSE (°C)	MAE (°C)	R²	RMSE (°C)	MAE (°C)	R²
(1)	Time	Pavement mean temperature (°C)	MLR(1)	2.13	1.75	0.68	2.10	1.70	0.42
(2)	Time and temperature of influent	Pavement mean temperature (°C)	MLR(2)	2.07	1.71	0.70	1.95	1.65	0.56
(3)	Time, temperature of influent and air temperature	Pavement mean temperature (°C)	MLR(3)	2.06	1.69	0.70	2.01	1.69	0.54
(4)	Time, temperature of influent, air temperature and temperature of effluent	Pavement mean temperature (°C)	MLR(4)	1.94	1.56	0.74	1.95	1.62	0.60
(1)	Time	Pavement mean temperature (°C)	MLP(1,1,1), *netinv-purelin*	2.14	1.77	0.68	1.93	1.71	0.42
(2)	Time and temperature of influent	Pavement mean temperature (°C)	MLP(2,1,1), *netinv-purelin*	2.09	1.74	0.69	1.64	1.32	0.65
(3)	Time, temperature of influent and air temperature	Pavement mean temperature (°C)	MLP(3,1,1), *netinv-purelin*	2.10	1.73	0.69	1.68	1.37	0.64
(4)	Time, temperature of influent, air temperature and temperature of effluent	Pavement mean temperature (°C)	MLP(4,1,1), *netinv-purelin*	1.82	1.49	0.77	2.06	1.82	0.46
(1)	Time	Pavement mean temperature (°C)	RBNN(1,0.1,14)	2.39	1.98	0.76	3.09	2.49	0.32
(2)	Time and temperature of influent	Pavement mean temperature (°C)	RBNN(2,0.5,2)	1.65	1.35	0.80	1.62	1.21	0.66
(3)	Time, temperature of influent and air temperature	Pavement mean temperature (°C)	RBNN(3,0.7,3)	1.95	1.63	0.73	1.56	1.10	0.70
(4)	Time, temperature of influent, air temperature and temperature of effluent	Pavement mean temperature (°C)	**RBNN(4,1.4,20)***	**0.59**	**0.46**	**0.97**	**1.27**	**1.07**	**0.77**

*indicates that the model has the best performance according to the RMSE and MAE.

Where N denotes the number of observations; Y indicates the modeled and measured pavement mean temperature, and $\overline{Y}$ indicates the mean of pavement mean temperature. The results of the MLR method were examined by Gevrek [15]. In this present study, MLP and RBNN methods are used and compared with the results of the MLR method. Table 3 shows the results of MLR, MLP, and RBNN models and RMSE, MAE and R^2 values in the training and testing phases for sample-1. In this table, the RBNN model of four inputs has a better performance than the other models. The MLP models had similar performance with the MLR models according to RMSE, MAE, and R^2 criteria in the testing phase. The RBNN models in the testing phase gave better estimations than MLR and MLP models. It can be said that the temperature of effluent and the temperature of influent are effective variables in estimating pavement mean temperature (°C).

Table 4 shows the results of MLR, MLP, and RBNN models and RMSE, MAE, and R^2 values in the training and testing phases for sample-2. In this table, the RBNN model of four inputs

Table 4- RMSE, MAE and R^2 values of the MLR, MLP, and RBNN in training and testing phase for sample-2

Comb. No.	Inputs	Target (output)	Model and optimum transfer function	Training (N=241)			Testing (N=104)		
				RMSE (°C)	MAE (°C)	R^2	RMSE (°C)	MAE (°C)	R^2
(1)	Time	Pavement mean temperature (°C)	MLR(1)	2.15	1.69	0.77	2.29	1.79	0.47
(2)	Time and temperature of influent	Pavement mean temperature (°C)	MLR(2)	1.98	1.61	0.80	1.72	1.40	0.71
(3)	Time, temperature of influent and air temperature	Pavement mean temperature (°C)	MLR(3)	1.97	1.60	0.81	1.71	1.37	0.72
(4)	Time, temperature of influent, air temperature and temperature of effluent	Pavement mean temperature (°C)	MLR(4)	1.96	1.61	0.81	1.73	1.37	0.71
(1)	Time	Pavement mean temperature (°C)	MLP(1,1,1), *netinv-purelin*	2.18	1.72	0.76	2.59	2.28	0.47
(2)	Time and temperature of influent	Pavement mean temperature (°C)	MLP(2,1,1), *netinv-purelin*	2	1.64	0.80	2.10	1.71	0.72
(3)	Time, temperature of influent and air temperature	Pavement mean temperature (°C)	MLP(3,1,1), *netinv-purelin*	2.01	1.65	0.79	2.07	1.71	0.76
(4)	Time, temperature of influent, air temperature and temperature of effluent	Pavement mean temperature (°C)	MLP(4,1,1), *tansig-purelin*	1.81	1.47	0.83	2.34	1.98	0.55
(1)	Time	Pavement mean temperature (°C)	RBNN(1,0.2,1)	3.6	2.91	0.36	2.52	2.23	0.34
(2)	Time and temperature of influent	Pavement mean temperature (°C)	RBNN(2,0.4,5)	1.19	0.95	0.93	1.74	1.42	0.80
(3)	Time, temperature of influent and air temperature	Pavement mean temperature (°C)	RBNN(3,1,8)	0.98	0.75	0.95	1.54	1.21	0.86
(4)	Time, temperature of influent, air temperature and temperature of effluent	Pavement mean temperature (°C)	**RBNN(4,0.8,7)***	**0.82**	**0.65**	**0.97**	**1.06**	**0.86**	**0.94**

* indicates that the model has the best performance according to the RMSE and MAE.

had better performance than the other models. MLP models had similar performance with the MLR models according to RMSE, MAE, and R^2 criteria in the testing phase. The RBNN models in the testing phase gave better estimations than MLR and MLP models. It can be said that the temperature of effluent and the temperature of influent are effective variables in estimating pavement mean temperature (°C).

Table 5 shows the results of MLR, MLP, and RBNN models and RMSE, MAE, and R^2 values in the training and testing phases for sample-3. In this table, the RBNN model of four inputs

Table 5- RMSE, MAE and R^2 values of the MLR, MLP, and RBNN in training and testing phase for sample-3

Comb. No.	Inputs	Target (output)	Model and optimum transfer function	Training (N=241)			Testing (N=104)		
				RMSE (°C)	MAE (°C)	R^2	RMSE (°C)	MAE (°C)	R^2
(1)	Time	Pavement mean temperature (°C)	MLR(1)	2.19	1.77	0.71	1.89	1.71	0.52
(2)	Time and temperature of influent	Pavement mean temperature (°C)	MLR(2)	2.18	1.77	0.71	1.89	1.71	0.52
(3)	Time, temperature of influent and air temperature	Pavement mean temperature (°C)	MLR(3)	2.09	1.59	0.73	1.77	1.54	0.57
(4)	Time, temperature of influent, air temperature and temperature of effluent	Pavement mean temperature (°C)	MLR(4)	1.90	1.41	0.78	1.67	1.34	0.74
(1)	Time	Pavement mean temperature (°C)	MLP(1,1,1), *logsig-purelin*	2.18	1.78	0.71	1.74	1.20	0.53
(2)	Time and temperature of influent	Pavement mean temperature (°C)	MLP(2,1,1), *logsig-purelin*	1.63	1.36	0.84	1.80	1.25	0.49
(3)	Time, temperature of influent and air temperature	Pavement mean temperature (°C)	MLP(3,1,1), *netinv-purelin*	2.15	1.64	0.72	2.01	1.52	0.53
(4)	Time, temperature of influent, air temperature and temperature of effluent	Pavement mean temperature (°C)	MLP(4,1,1), *logsig-purelin*	1.71	1.24	0.86	1.71	1.24	0.58
(1)	Time	Pavement mean temperature (°C)	RBNN(1,0.1,3)	2.3	1.85	0.68	2.12	1.71	0.42
(2)	Time and temperature of influent	Pavement mean temperature (°C)	RBNN(2,0.8,3)	1.64	1.36	0.83	1.64	1.35	0.48
(3)	Time, temperature of influent and air temperature	Pavement mean temperature (°C)	RBNN(3,1,8)	1.99	1.61	0.76	1.56	1.27	0.55
(4)	Time, temperature of influent, air temperature and temperature of fluent	Pavement mean temperature (°C)	**RBNN(4,0.6,9)***	**0.54**	**0.42**	**0.98**	**0.76**	**0.63**	**0.91**

* indicates that the model has the best performance according to the RMSE and MAE.

had better performance than the other models. MLP models had similar performance with the MLR models according to RMSE, MAE, and R^2 criteria in the testing phase. RBNN models in the testing phase gave better estimations than MLR and MLP models. It can be said that the temperature of effluent and the temperature of influent are effective variables in estimating pavement mean temperature (°C).

Table 6 shows the results of MLR, MLP, and RBNN models and RMSE, MAE, and R^2 values in the training and testing phases for sample-4. In this table, the RBNN model of four inputs had better performance than the other models. The MLP models were similar performance with the MLR models according to RMSE, MAE, and R^2 criteria in the testing phase. The RBNN models in testing phase gave better estimations than MLR and MLP models. It can be said that the temperature of effluent and temperature of influent are effective variables in estimating pavement mean temperature (°C).

Table 6- RMSE, MAE and R^2 values of the MLR, MLP, and RBNN in training and testing phase for sample-4

Comb. No.	Inputs	Target (output)	Model and optimum transfer function	Training (N=241)			Testing (N=104)		
				RMSE (°C)	MAE (°C)	R^2	RMSE (°C)	MAE (°C)	R^2
(1)	Time	Pavement mean temperature (°C)	MLR(1)	2.84	2.37	0.67	3.11	2.81	0.29
(2)	Time and temperature of influent	Pavement mean temperature (°C)	MLR(2)	2.58	2.16	0.73	2.65	2.48	0.53
(3)	Time, temperature of influent and air temperature	Pavement mean temperature (°C)	MLR(3)	2.46	1.98	0.75	2.58	2.35	0.54
(4)	Time, temperature of influent, air temperature and temperature of effluent	Pavement mean temperature (°C)	MLR(4)	1.99	1.58	0.84	1.88	1.73	0.78
(1)	Time	Pavement mean temperature (°C)	MLP(1,1,1), *tribas-purelin*	2.62	2.05	0.72	3.21	2.24	0.26
(2)	Time and temperature of influent	Pavement mean temperature (°C)	MLP(2,1,1), *netinv-purelin*	2.60	2.16	0.72	2.01	1.79	0.67
(3)	Time, temperature of influent and air temperature	Pavement mean temperature (°C)	MLP(3,1,1), *netinv-purelin*	2.51	2.04	0.74	1.97	1.62	0.65
(4)	Time, temperature of influent, air temperature and temperature of effluent	Pavement mean temperature (°C)	MLP(4,1,1), *netinv-purelin*	1.87	1.45	0.86	2.51	1.94	0.72
(1)	Time	Pavement mean temperature (°C)	RBNN(1,0.1,14)	2.39	1.98	0.77	3.09	2.49	0.32
(2)	Time and temperature of influent	Pavement mean temperature (°C)	RBNN(2,0.9,3)	2.10	1.70	0.82	1.66	1.45	0.79
(3)	Time, temperature of influent and air temperature	Pavement mean temperature (°C)	RBNN(3,1.7,18)	0.83	0.62	0.97	1.42	1.19	0.83
(4)	Time, temperature of influent, air temperature and temperature of effluent	Pavement mean temperature (°C)	**RBNN(4,1.5,8)***	**1.28**	**0.96**	**0.93**	**1.07**	**0.86**	**0.91**

* indicates that the model has the best performance according to the RMSE and MAE.

Table 7 shows the comparison of the best models for all samples in the testing phase. In this table, the RBNN models with four inputs had the best performance for each sample. RBNN(4,0.6,9) model, which is 4-inputs, spread coefficient of 0.6 and hidden nodes of 9 of sample-3, had the best performance among all models. When the other models were examined, it can be said that the RMSE and MAE error values were close to each other. It can also be said that the results of the models gave similar results in all four experimental samples. In general, the longer the T (heating time) is, the more other variables affect the pavement surface temperature. For example, the temperature of influent and temperature of effluent were effective variables in the models because they decreased the RMSE and MAE values of the models. According to the MAE values, it was seen that the error values were close to each other. The difference between the maximum MAE (1.07) and minimum MAE (0.63) was found to be 1.07-0.63 = 0.44 °C, which is quite low value for 104 data in the testing phase.

Table 7- Comparison of the best models for all samples in testing phase (N=104)

Inputs	Target (output)	The number of the inputs in the models	Samples	Model	RMSE (°C)	MAE (°C)	R^2
Time, temperature of influent, air temperature and temperature of effluent	Pavement mean temperature (°C)	4	Sample-1	RBNN(4,1.4,20)	1.27	1.07	0.77
Time, temperature of influent, air temperature and temperature of effluent	Pavement mean temperature (°C)	4	Sample-2	RBNN(4,0.8,7)	1.06	0.86	0.94
Time, temperature of influent, air temperature and temperature of effluent	Pavement mean temperature (°C)	**4**	**Sample-3**	**RBNN(4,0.6,9)***	**0.76**	**0.63**	**0.91**
Time, temperature of influent, air temperature and temperature of effluent	Pavement mean temperature (°C)	4	Sample-4	RBNN(4,1.5,8)	1.07	0.86	0.91

* indicates that the model has the best performance according to the RMSE and MAE.

The best models, (a)RBNN(4,1.4,20), (b)RBNN(4,0.8,7), (c)RBNN(4,0.6,9) and (d)RBNN(4,1.5,8) in Figure 6, are graphically compared in the form of time series according to the results of the testing phase. Scatter plots are also given in Figure 6 in which the measured pavement mean temperature in the x-axis and the modeled pavement mean temperature in the y-axis are depicted. It can be seen from Table 7 and the figures that the
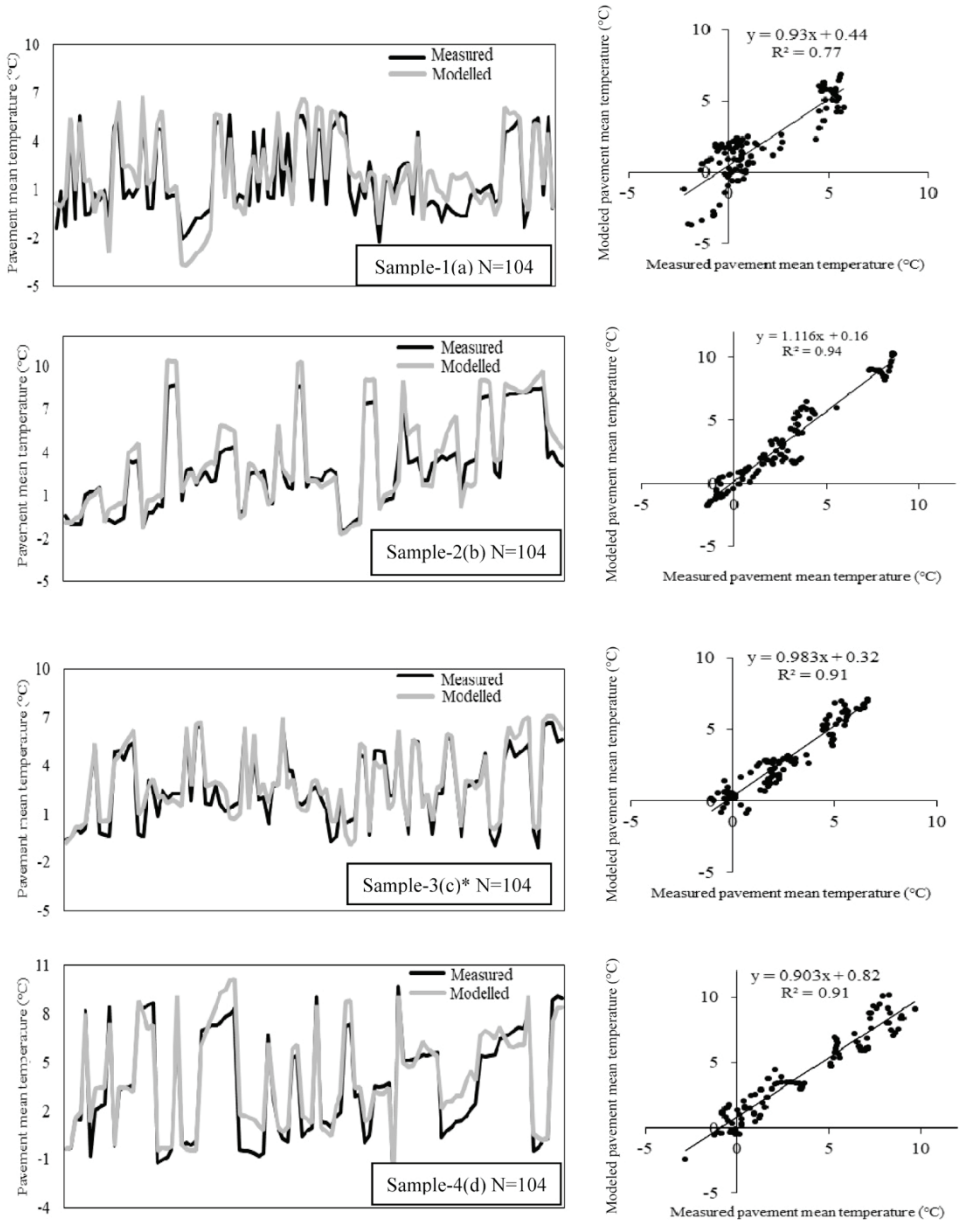
Figure 6 -The measured and modeled pavement mean temperature for the best models Sample-1(a) RBNN(4,1.4,20), Sample-2(b) RBNN(4,0.8,7), Sample-3(c) RBNN(4,0.6,9)* and Sample-4(d) RBNN(4,1.5,8) in the testing phase (N=104)

best model is RBNN(4,0.6,9) according to the evaluation criteria. Looking at the model results of four experimental examples, the methods generally have similar performance in terms of modeling of pavement mean temperature. In the four experimental examples, it was seen that the MLR models gave slightly better results than the MLP models in the testing phases. The RBNN method also gave similar results, which were the best models in four experimental examples. In this context, it can also be stated that the four asphalt samples behave similarly in the models in terms of experimental and modeling consistency.

5. CONCLUSIONS

After usability of the hydronic heating systems in snow and icing control in the pavements was investigated in Gevrek [15], the pavement mean temperature was modeled by using MLR, MLP, and RBNN methods. In this context, the performances of the models were evaluated using the model performance criteria of RMSE, MAE, and R^2. In view of the results obtained, the following conclusions can be drawn:

1. Preventing snow and ice on the surface of hydronic asphalt pavement could make a significant contribution to reducing traffic accidents and environmental damages and increases the highway capacity in extreme weather conditions.

2. Thermal stress-induced shrinkage of asphalt pavement layers, which is one of the important deterioration forms in winter can be reduced by using hydronic heating systems.

3. Traditional road maintenance costs, such as salting and snow removal, which might damage the structure could be reduced by using hydronic heating systems. At the same time, these systems can positively contribute to the highway pavement life cycle.

4. Considering the benefit/cost ratios and project design-construction works of hydronic heating systems, it can be said that these systems are significantly cost effective in terms of investment costs in order to maintain their engineering properties in future projections.

5. It was generally seen that the MLR models gave slightly better results than the MLP models in the testing phases for the four experimental examples.

6. The RBNN models with four inputs had the best performance for each asphalt sample. The RBNN (4,0.6,9) model of sample-3 with RMSE=0.76 °C and MAE=0.63 °C and R^2=0.91 for 104 testing data had the best performance among all models. According to these results, it can be said that the statistically obtained models can be used in early icing warning systems, and can contribute to rapid decision-making processes.

7. Considering the model results of four experimental examples, it can be said that the methods generally have similar performance in terms of modeling of pavement mean temperature. In this context, the four asphalt samples behaved similarly in the models in terms of experimental and modeling consistency.

8. In terms of significant impact on these laboratory samples, this system could be tested and modeled on a larger scale in real in-situ conditions. However, it was thought that starting from this point as the first study it would inform us in terms of guiding our studies in the future.

9. It is recommended that some further analyses should be made using other artificial intelligence applications to find better estimates for the asphalt pavement surface temperature.

10. In the study, it was determined that the correlation coefficient increased significantly with the inclusion of the inlet water temperature in the model. As a result, it can be concluded that the inlet water temperature should be increased in order to increase the asphalt surface temperature. It has been shown that 40°C water can be a sufficient temperature for such systems to be used for snow and ice prevention purposes [39]. It can be made energy efficient by making use of waste heat sources from electricity and residential heating from renewable sources such as geothermal sources, where high temperatures are not needed.

Symbols

MAE	Mean absolute error
MLR	Multiple linear regression
MLP	Multi-layer perceptron
RBNN	Radial basis neural network
RMSE	Root mean square error
R²	Determination coefficient
r	Correlation coefficient
T	Time

References

[1] Fay, L., Volkening, K., Gallaway, C., Shi, X., Performance and Impacts of Current Deicing and Anti-Icing Products: User Perspective versus Experimental Data. Presented at 87th Annual Meeting of the Transportation Research Board, Washington DC., 08-1382, 2008.

[2] Houssain, SMK., Optimum De-Icing and Anti-Icing for Snow and Ice Control of Parking Lots and Sidewalks. PhD thesis in Civil Engineering. The University of Waterloo, 186, Canada, 2014.

[3] Adl-Zarrabi, B., Mirzanamadi, R., Jhonsson, J., Hydronic Pavement Heating for Sustainable Ice-free Roads. Transportation Research Procedia, 14, 704-713, 2016.

[4] Akbulut, H., Woodside, AR., Traffic Safety and Unprotected Road Users in Low and Middle Income Countries. Journal of Innovations in Civil Engineering and Technology, 1(1), 1-9, 2019.

[5] Blomqvist, S. Amiri, S. Rohdin, P. Ödlund, L., Analyzing the Performance and Control of a Hydronic Pavement System in a District Heating Network. Energies, 12(11), 2078, 2019.

[6] Feng, J., Yin, G., Thermal Analyses and Responses of Bridge Deck Hydronic Snow Melting System. Advances in Civil Engineering. 8172494, 14p, 2019.

[7] ASHRAE, Handbook of HVAC Applications, American Society of Heating, Refrigerating and Air-Conditioning Engineers, Inc, Atlanta, GA, 2003.

[8] Ho, I-H., Li, S., Abudureyimu, S., Alternative Hydronic Pavement Heating System Using Deep Direct Use of Geothermal Hot Water. Cold Regions Science and Technology, 160, 194-208, 2019.

[9] Liu X., Spitler J.D., A Simulation Tool for the Hydronic Bridge Snow Melting System, 12th International Road Weather Conference, 2003.

[10] Anand, P., Nahvi, A., Ceylan, H., Pyrialakou, V.D., Gkritza, K., Gopalakrishnan, K., Kim, S., Taylor, PC., Energy and Financial Viability of Hydronic Heated Pavement Systems, National Technical Information Services (NTIS), Springfield, Virginia 22161, No. DOT/FAA/TC17/47, 2007.

[11] Lund, JW., Pavement Snow Melting. Geo-Heat Center Quarterly Bulletin, 21(2), 12-19, 2000.

[12] Fujimoto, A., Tokunaga, RA., Kiriishi, M., Kawabata, Y., Takahashi Ishida, T., Fukuhara, T., A road surface freezing model using heat, water and salt balance and its validation by field experiments. Cold Reg. Sci. Technol., 106-107, 01-10, 2014.

[13] Akbulut, H., Gürer, C., Gevrek, L., Highway Pavement Surface Icing and Traffic Safety. International Journal of Scientific Engineering Research, 9(8), 6-9, 2018.

[14] Xu, H., Wang, D., Tan, Y., Zhou, J., Oeser, M., Investigation of design alternatives for hydronic snow melting pavement systems in China. Journal of Cleaner Production, 170, 1413-1422, 2018.

[15] Gevrek Atılgan, L., Modeling of Anti-Icing Systems with Geothermal Energy in Highway Pavements. Afyon Kocatepe University, Graduate School of Natural and Applied Sciences, PhD Thesis, Turkey, 2021.

[16] Gustafson, K., Icing Conditions on Different Pavement Structures. Transportation Research Record 860. Nr 84, ISSN 0347-6049, 1983.

[17] Xiao, J., Kulakowski, BT., El-Gindy, M., Prediction of Risk of Wet-Pavement Accidents: Fuzzy Logic Model. Transportation Research Record, 1717(1), 2000.

[18] Eugster, WJ., Road and Bridge Heating Using Geothermal Energy Overview and Examples. Proceedings European Geothermal Congress, Unterhaching, Germany, 30 May-1 June, 2007.

[19] Chiasson, AD., Spitler, JD., Rees, SJ., Smith, MD., A model for simulating the performance of a pavement heating system as a supplemental heat rejecter with closed-loop ground-source heat pump systems. Journal of Solar Energy Engineering, 122(4), 183-191, 2000.

[20] Minhoto, MJC., Pais, JC., Pereira, PAA., Picado-Santos, LG., Predicting asphalt pavement temperature with a three-dimensional finite element method. Transp. Res. Rec., 1919(1), 96-110, 2005.

[21] Liu, X., Rees SJ., Spitler, JD., Modeling snow melting on heated pavement surfaces. Part I: Model development. App Therm Eng, 27, 1115-1124, 2007a.

[22] Liu, X., Rees SJ., Spitler, JD., Modeling snow melting on heated pavement surfaces, Part II: Experimental validation. App Therm Eng, 27, 1125-1131, 2007b.

[23] Wang, H., Chen, Z., Study of critical free-area ratio during the snow-melting process on pavement using low-temperature heating fluids. Energy Conversion and Management, 50(1), 157-165, 2009.

[24] Xu, H., Tan, Y., Modeling and Operation Strategy of Pavement Snow Melting Systems Utilizing Low-Temperature Heating Fluids. Energy, 80, 666-676, 2015.

[25] Mirzanamadi, R., Hagentoft, CE., Johansson, P., Johnsson, J., Anti-icing of Road Surfaces Using Hydronic Heating Pavement with Low Temperature. Cold Regions Science and Technology, 145, 106-118, 2018.

[26] Jhonsson, J., Adl-Zarrabi, B., Modeling the thermal performance of low temperature hydronic heated pavements. Cold Regions Science and Technology, 161, 81-90, 2019.

[27] Chen, J., Wang, H., Xie, P., Pavement temperature prediction: theoretical models and critical affecting factors. Applied Thermal Engineering, 158, 113755, 2019.

[28] Zeiada, W., Hamad, K., Omar, M., Underwood, BS., Khalil, MA., Karzad, AS., Investigation and modelling of asphalt pavement performance in cold regions. International Journal of Pavement Engineering, 20(8), 986-997, 2019.

[29] Mirzanamadi, R., Hagentoft, CE., Johansson, P., Coupling a Hydronic Heating Pavement to a Horizontal Ground Heat Exchanger for harvesting solar energy and heating road surfaces. Renewable Energy,147(Part 1), 447-463, 2020.

[30] Zhao, W., Su, W., Li, L., Zhang, Y., Li, B., Optimization design of the road unit in a hydronic snow melting system with porous snow. Journal of Thermal Analysis and Calorimetry, 141, 1509-1517, 2020.

[31] Marcelino, P., Antunes, MDL., Fortunato, E., Gomes, MC., Machine learning approach for pavement performance prediction. International Journal of Pavement Engineering, 22(3), 341354, 2021.

[32] Rigabadi, A., Herozi, MRZ., Rezagholilou, A., An attempt for development of pavements temperature prediction models based on remote sensing data and artificial neural network. International J of Pavement Engineering, 23(9), 2912-2921, 2021.

[33] Tabrizi, SE., Xiao, K., Thè, JVG., Saad, M., Farghaly, H., Yang, SX., Gharabaghi, B., Hourly road pavement surface temperature forecasting using deep learning models. Journal of Hydrology, 603, Part A, 126877, 2021.

[34] Ay, M., Kisi, Ö., Modelling of chemical oxygen demand by using ANNs, ANFIS and k-means clustering techniques. Journal of Hydrology, 511, 279-289, 2014.

[35] Haykin, S., Neural networks: A comprehensive foundation. 2nd Ed., Prentice-Hall, Upper Saddle River, NJ., 1998.

[36] Marquardt, D., An algorithm for least squares estimation of nonlinear parameters. J. Soc. Ind. Appl. Maths., 11(2), 431-441, 1963.

[37] Broomhead, D., Lowe, D., Multivariable functional interpolation and adaptive networks. Complex Syst., 2(6), 321-355, 1988.

[38] Poggio, T., Girosi, F., Regularization algorithms for learning that are equivalent to multilayer networks. Science, 247(4945), 978-982, 1990.

[39] Wang, H., Zhao, J., Chen, Z., Experimental Investigation of Ice and Snow Melting Process on Pavement Utilizing Geothermal Tail Water. Energy Conversion and Management, 49, 1538-1546, 2008.